Larhyss Journal, ISSN 1112-3680, n°57, Mars 2024, pp.209-239

AN EXPERIMENTAL STUDY ON THE VARIATION OF SCOUR DEPTH FOR DIFFERENT PIER SHAPES USING A TILTING FLUME

DALAL B., DEB S.*

Department of Civil Engineering, ICFAI University Tripura, India-799210

(*) subhrajyotideb@iutripura.edu.in

Research Article – Available at http://larhyss.net/ojs/index.php/larhyss/index
Received October 12, 2023, Received in revised form February 25, 2024, Accepted February 27, 2024

ABSTRACT

The investigation of scour near bridge piers has substantial importance in guaranteeing the secure and efficient design of the structure. The term "scouring phenomenon" pertains to the process of erosion and elimination of bed particles situated in close proximity to the bridge pier. The objective of this study is to examine the depth of local scour in the vicinity of six different pier forms, specifically circular, rectangular, sharp-nosed, oblong, joukowsky, and chamfered. The aim of this study is to ascertain the most efficient and economically viable design for bridge piers. The experiment encompasses a range of discharges and velocities, specifically ranging from 0.00104 cumecs to 0.00157 cumecs and from 0.22 meters per second to 0.33 meters per second, respectively. The study's results suggest that the presence of a horseshoe vortex contributes to the increased amplitude of scour at the rectangular bridge pier. In contrast, the depth of scour in the vicinity of the pointed nose pier is reduced due to the bifurcation of flow resulting from its streamlined contour. Furthermore, the model is simulated via the HEC-RAS modeling software. The correlation between the depths of scour measured in my experiment and the depth of scour predicted by three different numerical models has been established. The results of this study have the capacity to provide valuable insights for the decision-making process regarding the selection of bridge pier designs. The findings indicate that the sharp nose pier shape exhibits superior performance in terms of both safety and serviceability compared to the other five pier shapes.

Keywords: Local scour, pier shape, sediment transport, flume test, HEC-RAS

INTRODUCTION

Bridges over rivers are the most prominent kind of physical communication infrastructure in a nation (Ghasemi Asl and Heidarnejad, 2023). In contemporary society, bridges play a vital role as the primary infrastructure supporting a nation's transit network. To enhance the country's infrastructure, it is essential to construct a substantial quantity of railway

and road bridges over various rivers, streams, and bodies of water. Furthermore, the potential ramifications associated with the structural failure of the bridge might be significant. The main reasons attributed to bridge collapses are determined to be local scour (64%), channel migration (13%), and contraction scour (6%). In contrast, the occurrence of scouring and contraction is shown to be less prevalent, according to Chavan (2021). According to the findings of Bian et al (2023), a significant number of bridges, over 1,000, have experienced collapse in the United States during the preceding three decades. It has been shown that around 60% of these collapses may be attributed to the scour of bridge foundations, as stated by Karimi et al (2020). The study done by Rafiqui et al (2023) reveals that the scouring phenomenon occurring around bridge pier foundations is recognized as a primary cause of a notable bridge collapse in New Zealand. According to the findings of Wang et al (2023), a total of 155 bridges in China experienced a collapse, mostly attributed to two primary factors. The first factor pertains to issues related to the foundations, which constituted around 20% of all recorded collapses. The second factor is associated with floods and scour events. The collapse of the Mumbai-Goa Highway Bridge in India was attributed to the significant rainfall experienced in the region. The fundamental cause of the bridge's failure seems to be the elevated pressure resulting from flooding in the Savitri River and excessive rainfall in the Mahabaleshwar watershed area, which led to the erosion and subsequent collapse of the British-built bridge in Mahad (Mehta et al. 2020).

The term "scour" refers to the process of bed sediment erosion occurring near an obstruction in a fluid flow environment. Breusers et al. (1977) define "scouring" as sediment displacement on river and stream bottoms where hydrodynamic forces of water flow cause displacement. According to many studies (Richardson et al. 2001; Qaderi et al., 2021; Rafiqui, 2023; Choi, 2021), local scour contributes to hydraulic structural collapse, Vijayasree et al. (2019) explored how the main horseshoe vortex affects scouring near a cylindrical pier and discovered that the vortex drives the scouring phenomenon throughout the operation. Raudkivi and Witte (1990), Singh et al. (2020), Rafiqui et al. (2023), Breusers et al. (2020), Richardson and Davis (2001), Xu et al. (2023), Shahriar et al. (2021), Tang et al. (2023), and Fleit et al. (2023) demonstrate the large literature on local scour at bridge piers. According to the research, flow disruptions create a substantial pressure field at the bridge pier, when the pressure field hits a threshold, the boundary layer separates, creating three-dimensional phenomena. On the opposite side of the pier from the upstream flow, a major vortex forms when fluid velocity in a channel is limited to the downward direction. Figure 1 shows a horseshoe vortex, referred to as such because the river flows under the bridge's piers and creates vortices (Richardson et al. 2001). Local scour occurs when fluid flow accelerates, causing vortices that restrict flow which begins near the pier and continues to the downstream. Wake vortices enhance lateral and vertical flow near the pier, causing scouring downstream. The pier's wake vortices' proportions and intensity depend on the fluid flow velocity and its size and shape. According to Richardson and Davis (2001), a wake vortex's strength decreases downstream from a pier, causing silt to accumulate near the pier. As the scour hole deepens, the vortices at the pier foundation weaken, establishing equilibrium. Bed material outflow stops at this equilibrium.

The hydrodynamic forces of moving water displace silt from the fluvial bed during "general scouring". Local scour around bridge foundations, including piers and abutments, is a major factor in bridge damage and failure. Jia et al. (2018) found that local scour erodes bed sediment near the bridge pier, which reduces the foundation's lateral capacity. Jalal et al. (2020) define "local scour" as soil erosion caused by hydraulic forces from water moving near an obstacle in engineering applications. The vertical decline of fluid motion at the pier's closest face causes localized scouring around bridge piers. The downward flow in this scenario creates vortices around the pier base. Local scour in cohesion-less soil is classified as clear-water (CWS) or live-bed (LBS). Clear-water scour (CWS) occurs when upstream material cannot be effectively carried by the upstream approach flow, preventing it from accumulating in the scour hole and it gradually increases until equilibrium. In Localized Bed Scour (LBS), approach flow sustains silt entry into the scour hole. Local Scour at Bridge Structures (LBS) shows that vortex velocity and intensity exceed sediment bed shear strength. The scour hole grows due to pressure differences. The inverse relationship between sediment intake and outflow drives scour depth variation in the scour hole, culminating in equilibrium stabilization. Clear-water scour (CWS) occurs when the incoming flow velocity (V) is equal to or below the critical velocity (V_c), represented as ($V \leq V_c$). Alternatively, live bed scouring (LBS) occurs when the velocity (V) surpasses the critical velocity (V_c), symbolized as ($V > V_c$), when sediment intake matches sediment outflow from the scour hole. The LBS's scour depth varies, but the average depth is consistent.

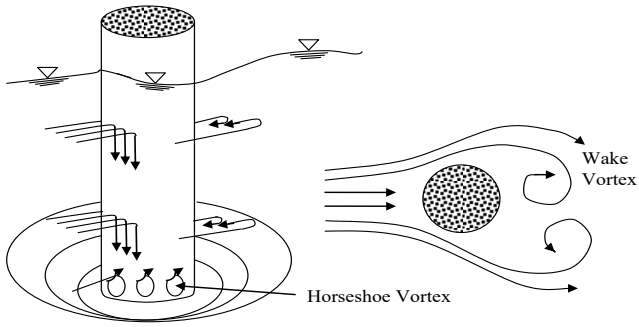

Figure 1: Illustration of wake and horseshoe vortices that form around a circular bridge pier (Richardson and Davis 2001)

When confronted with the complexities of distinguishing between Cross-Wave Speed (CWS) and Longitudinal Bed Slope (LBS), the establishment of critical velocity can be achieved by employing equation (1) as postulated by Dou (1997) and cited in HEC-18 by Richardson et al (1993).

$$V_c = 6.36 y^{1/6} d_{50}{}^{1/3} \tag{1}$$

The fluid flow dynamics are greatly affected by the existence of a non-circular pier that is buried in a sediment bed. This alteration introduces complications in accurately predicting the depth of scour. Hence, more empirical inquiries are necessary in order to

obtain a full comprehension of the inherent flow phenomena linked to a bridge pier exhibiting a non-circular form, including rectangular, chamfered, sharp nosed, joukowsky and oblong configurations (Mowla et al., 2024).

The current work aims to make a significant contribution to the collection of diverse data sets. The prior study is deficient in terms of the quantity of experimental data sets available for the various layouts of bridge piers. Experimental studies have been conducted to expand the current data set with the aim of predicting scour depth and gaining a comprehensive knowledge of flow dynamics associated with various designs of bridge piers. This research paper outlines an experimental study that was carried out to accurately measure the depths of local scour for six different kinds of bridge piers. The research involves gathering data from empirical investigations that relate to the above factors. The newly created model is analyzed using the HEC-RAS modeling tool, together with the depth of scour prediction formulae proposed by CSU (1975) and Breusers et al (1977), represented by equations 4 and 6, respectively. The findings of this comparison are thereafter presented clearly in the Results and Analysis section.

LITERATURE REVIEW

The examination of local scour in rivers was first undertaken by Tison (1961) through laboratory experiments. Various bridge pier models with varying forms, such as aerodynamic, lens-shaped, triangular, and rectangular designs, were utilized in these tests. The phenomenon of local scouring in the area of bridge piers was comprehensively investigated by Guan et al (2022). The researchers systematically manipulated many elements, including the size of the grains, pier diameter, water level, and pier design, in order to get a more thorough understanding of this phenomenon. Abutments can modify sedimentation and deposition, either encouraging protective sediment layers or exacerbating scour depth. The hydraulic forces around abutments, particularly during high-flow events, contribute to the complexity of their influence on scour depth. In a study Zolghadr et al. (2023) aimed to assess the efficacy of using roughening features as a potential mitigation strategy against bridge abutment scour. The study investigated two vertical wall abutments of varying widths across four distinct hydraulic situations inside a clear-water regime. According to their research findings, the optimal configuration (P = t = 0.2 L and Z = >0.6–0.8 L) resulted in a reduction of the maximum scour depth by about 30.4% and 32.8% for the abutment with narrower and wider widths, respectively. The achievement of a steady scour depth state has been seen when the velocities of fluids decreased below the critical rate required for particle motion. At this juncture, the scour depth reaches its utmost magnitude. The scour depth experiences fluctuations at higher velocities as a result of the periodic deposition of sediment in the places of the scour hole. The influence of the position and shape of a single bridge pier on the equilibrium of depth of scour was explored by Fael et al. (2016) in their research. This investigation was conducted under conditions of clear water flow, namely at the threshold when sediment motion begins. The study investigated five unique bridge pier designs, each characterized by varying form proportions. Achour et al. (2022) provide a comprehensive theoretical framework for determining the backwater curves that develop in a triangular channel. In

the context of the C1-type backwater curve, a novel expedited approach is introduced, enabling the straightforward computation of the distance between two specified depths. Achour et al (2022) thoroughly investigate the impact of the configuration of a broad-crested weir on the density of a rectangular stilling basin. The study's findings are derived from meticulously performed experimental experiments conducted under different incident flow circumstances. A custom-designed hydraulic system was used for this specific application. In their study, Achour et al (2022) address the issue of determining the optimal value of the sill location X in order to get a fully formed hydraulic jump on the stilling basin, with a length L_j that is nearly equal to X. According to the study conducted by Escauriaza et al (2023), the authors suggest that the existence of obstacles disrupts the movement of fluid, leading to an increase in the bed shear stress and turbulence intensity in the immediate vicinity. Consequently, this enables the movement of silt deposited on the bed. The investigation carried out by Harasti et al (2021) focused on the analysis of scouring occurrences in the vicinity of bridge piers inside rivers experiencing flooding events. The results of the study indicated a negative correlation between the size of particles in river silt and the extent of local scouring. It was observed that an increase in particle size corresponded to a decrease in depth of scour. This observation implies that the scouring process is influenced by the properties of the bed surface, wherein the presence of fine sand bed levels leads to a notable increase in scouring. The study undertaken by Jueyi et al. (2010) involved the measurement of scouring phenomena near semi-elliptical abutments that were fitted with armored beds. The experiments were carried out under conditions of clear water scour (CWS). The research performed an analysis of the local scour phenomena near piers, followed by a comparison of the findings with those seen in semi-circular abutments. Based on the existing literature, it has been noted that an increase in flow velocity results in an elevation of both the scour hole and the equilibrium depth of scour in semi-elliptical and semi-circular abutments. Li et al (2023) conducted a research to quantify the depth of scour around a pier in the presence of clear-water scour (CWS) using different sediment mixtures. The study's findings suggest that bridge pier scour arises as a result of the interplay between flow dynamics, structural attributes, and sediment properties. The phenomenon of flow-structure interaction is accountable for the generation of vortices in the vicinity of a pier's base, therefore exerting a significant influence on the determination of the equilibrium scour depth. Based on the findings of the study, a direct relationship has been seen between the extent of pier blockage and the equilibrium scour depth. Conversely, a negative association has been identified between sediment non-uniformity and the equilibrium scour depth. Abudallah et al (2021) conducted a research study aimed at investigating the scouring phenomena around bridge piers of different forms, including circular and elongated, and with and without pier slots. The study employed an experimental approach to analyze these variables. The research findings suggest that the use of piers equipped with slots, as opposed to piers without slots, leads to a notable decrease in the maximum depth of scours. The circular piers undergo a decrease of 26%, while the elongated piers see a drop of 16%. Al-Shukur et al (2016) performed calculations to ascertain the scour depth for 10 different pier configurations in their research study.

Table 1: The importance of the preceding research is in the provision of a diverse array of datasets pertaining to various bridge pier configurations

Pier shape	Research Work	Q (m^3/sec)	V (m/sec)	D_{50} (mm)	b (cm)	y (m)	y_s/b
Circular	Al-Shukur et al. (2016)	0.0109-0.018	0.18-0.30	0.71	4.5	0.12	0.866-1.533
Rectangular	Al-Shukur et al. (2016)	0.0109-0.018	0.18-0.30	0.71	4.5	0.12	0.955-1.688
Sharp-nosed	Al-Shukur et al. (2016)	0.0109-0.018	0.18-0.30	0.71	4.5	0.12	0.66-1.088
	Goswami (2013)	-	0.006-0.251	0.10-4.2	3.6	-	7.5-10.0
	Ebrahimi et al. (2018)	0.0191-0.334	-	1.37	5.0	8.0-13.1	4.87-11.0
Oblong	Al-Shukur et al. (2016)	0.0109-0.018	0.18-0.30	0.71	4.5	0.12	0.911-1.288
	Vijayasree and Eldho (2016)	0.012-0.018	0.36	0.80	3.0	0.165	0.047
Joukowsky	Al-Shukur et al. (2016)	0.0109-0.018	0.18-0.30	0.71	4.5	0.12	1.044-1.355
	Khassaf and Ahmed (2021)	0.0028-0.0048	0.16-0.27	0.4	4.5	0.03	-
Chamfered	Al-Shukur et al. (2016)	0.0109-0.018	0.18-0.30	0.71	4.5	0.12	0.9111-1.488
	Talib et al (2016)	0.0109-0.018	0.18-0.30	0.71	4.5	0.12	0.9111-1.488
	Khassaf and Ahmed (2021)	0.0028-0.0048	0.16-0.27	0.4	4.5	0.03	-

Based on available studies, it has been observed that the depth of scour surrounding the rectangular configuration of the pier is greater. Conversely, the streamlined pier has the opposite impact. The streamlined pier is frequently considered to be one of the most efficient pier configurations among the 10 regularly utilized varieties, mostly due to its lower vulnerability to scouring. The experimental investigation conducted by Okina et al. (2023) examined the effects of scouring on several pier geometries, such as diamond, circular, and elliptical shapes. The use of an elliptical-shaped pier, in contrast to a diamond-shaped pier, led to a decrease of around 15% in the magnitude of local scour. In the same manner, the use of an elliptical-shaped pier, as opposed to a pier with a circular form, resulted in a reduction of roughly 10% in the occurrence of local scour. In their empirical study, Helmy et al. (2017) performed an examination to analyze the incidence of local scour in the vicinity of piers of different forms, such as lenticular (curve), lenticular, hexagonal and elliptical. The trials were carried out in hydraulic channels with curved geometries, where the rate of flow (q) and inclined angle of the piers were manipulated to replicate conditions resembling clear water scour (CWS). The efficacy of

the lenticular (curved) configuration of the pier has been demonstrated to surpass that of the elliptical and hexagonal configurations in terms of providing protection. This phenomenon can be linked to the pier's capacity to reduce the formation of horseshoe vortices in its vicinity. Based on available studies, it has been observed that the utilization of non-traditional pier designs has exhibited enhanced performance when compared to conventional geometric shapes. Adib et al (2020) conducted a research to evaluate the local scour depth along piers using sharp nose and round nose designs for the El Minia and Aswan bridges in Egypt. The assessment was conducted with mathematical models inside both one-dimensional (1D) and two-dimensional (2D) frameworks. Based on extant scholarly investigations, there exists a proposition positing that bridge piers characterized by a pointed nose configuration demonstrate a diminished extent of scour depth. Therefore, it is recommended to employ a design approach for piers that incorporates consistent cross-sectional profiles and minimum dimensions as a means to alleviate the impact of local scour depth. Bor and Guney (2022) conducted a comprehensive study that included a combination of experimental and computational techniques to ascertain the local scour depth surrounding bridge piers with square geometries. Based on the claim, it is seen that a scour depth above 90% of the maximum value is observed in close proximity to the onset of peak flow times. The majority of studies investigating scour depth have employed physical models of bridge piers (Chiew, 1984; Lança et al., 2013; Tafarojnoruz et al., 2010; Wang et al., 2019; Omara et al., 2022; Bor and Guney, 2022; Ebrahimi et al., 2018; Chooplou et al., 2023). The dataset of several bridge pier forms, including sharp-nosed, rectangular, circular, oblong, joukowsky, and chamfered, is presented in Table 1. This comprehensive dataset has been acquired from the previous researcher.

The following academics have studied bridge piers that are oval, chamfered, sharp-nosed, or joukowsky in form.

1. Chamfered - Al-Shukur and Obeid (2016), and Khassaf and Ahmed (2021).
2. Joukowsky - Al-Shukur and Obeid (2016)
3. Oblong- Eldho et al, (2010), Al-Shukur and Obeid (2016), Fael et al (2016), Vijayasree and Eldho (2016), and Hassan et al (2022).
4. Sharp-nosed shape - Ettema et al (2006), Al-Shukur and Obeid (2016), Ebrahimi et al (2018).
5. Rectangular shape - Maza (1968), Parola et al (1996), Oliveto and Hager (2002), Al-Shukur and Obeid (2016), Fael et al (2016).
6. Circular shape - Shen et al (1969), Chiew (1984), Ettema et al (2006).

Therefore, there has been minimal research conducted on the Joukowsky, oblong, chamfered and sharp nose forms of bridge piers, with a restricted dataset accessible in prior literature (Ettema et al 2006, Al-Shukur et al 2016, Khassaf and Ahmed 2021). To address this gap, an experimental study was conducted to obtain a more comprehensive range of data on all six shapes of bridge piers. The main objective of this study is to examine the variation of scour depth with different shapes of pier. So it will give a clear idea about the effect of different shapes of pier on scour depth. Later, the experimental values are compared with the predicted scour depth values which are computed by HEC RAS modelling software.

METHODOLOGY

Laboratory setup

The trials were carried out at the Water Resources Engineering laboratory, which is located inside the Civil Engineering Department of the ICFAI University Tripura. The trials were performed inside a rectangular tilting flume that had dimensions of 6.0 m in length, 0.3 m in breadth, and 0.6 m in depth. The use of a tilting flume in the present experimental study offers several advantages. A tilting flume allows for simulating and controlling the water flow for systematic testing of various pier shapes under controlled conditions. This experimental setup provides valuable insights into the impact of pier shapes on scour depth across a range of conditions. In summary, the tilting flume was chosen for this study to facilitate controlled experimentation, allowing us to investigate the effects of different pier shapes on scour depth under varying flow scenarios. The flume had a constant slope of 0.0003 and was designed to function as an open channel, with the top side being open which is shown in figure 2. On both sides of the flume's walls, there were transparent Perspex sheets, allowing viewers to see the fluid flow near the piers. The sediment bad inside the flume is uniformly distributed and has been filled to a depth of 10.0 cm in order to properly embed the pier model. The piers are installed at a distance of 3 m from the upstream side of the flume. Piers significantly affect scour depth mainly through disruptions in local flow patterns and vortex formation. Sediment transport is also influenced, creating areas of accumulation or erosion. Engineers often employ countermeasures like riprap and scour blankets to mitigate scour effects and ensure stability, similar to approaches used for abutments.The experimental setup includes a tilting flume configuration, accompanied by the installation of a vertical gate to control the condition of the downstream water. An orifice is attached inside the pipe along with a manometer. A pictorial view of the experimental set-up of the Tilting flume used in the study is shown in figure 3. The pressure difference readings were taken with the help of manometer. The equation used for the computation of discharge is given in equation 2.

$$Q = \frac{a_1 a_2 \times \sqrt{2gh}}{\sqrt{{a_1}^2 - {a_2}^2}} \quad (2)$$

Where, a_1= area of pipe and a_2 = area of orifice

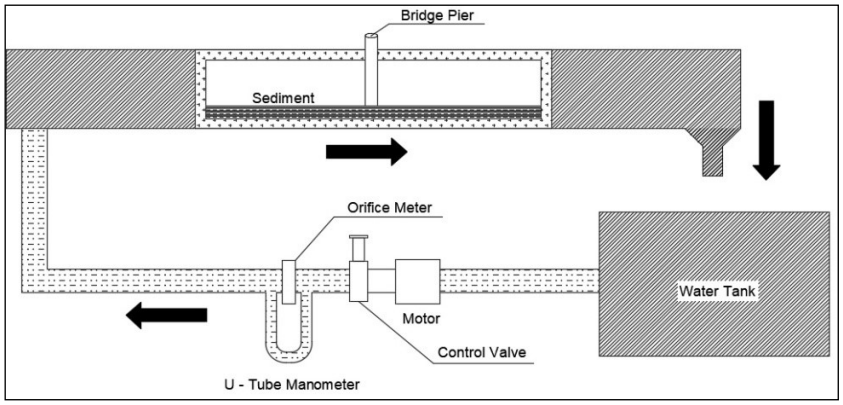

Figure 2: A diagram of the experimental setup (Rectangular tilting flume)

Figure 3: Experimental set-up of the Tilting flume used in the study

Figure 4: Various bridge pier types utilized in the experimental study. (Circular, rectangular, sharp-nosed, oblong, Joukowsky, and chamfered shapes)

Modeling of different pier shapes

The present study examines the effects of various bridge pier shapes on the depth of local scour. Specifically, six different shapes, including circular, rectangular, sharp-nosed, oblong, chamfered and joukowsky are investigated. Figure 4 illustrates these shapes. The study compares the predicted depth of local scour with the local scour prediction equations proposed by CSU (1975), HEC-RAS modeling tool, and Breusers et al (1977. The form of bridge piers consists of high-quality waterproof wood in order to prevent any expansion in the size of the piers due to swelling. In order to mitigate the interference of flow, it is recommended that the width of the pier should not exceed 12.5 percent of the width of the flume, as suggested by Chiew (1984) and Shen et al. (1966). The proportions of the bridge pier forms, encompassing rectangular, round, sharp-nosed, joukowsky, oblong, and chamfered shapes, were determined to have a uniform measurement of 3.0 cm apiece, with the circular shape having a diameter of 3.0 cm. The measurements were acquired with respect to the width of the flume, which was recorded as 30.0 cm. The aspect ratio of 4:1, as utilized by Al-Shukur and Obeid (2016), has been chosen for the present study due to its compatibility.

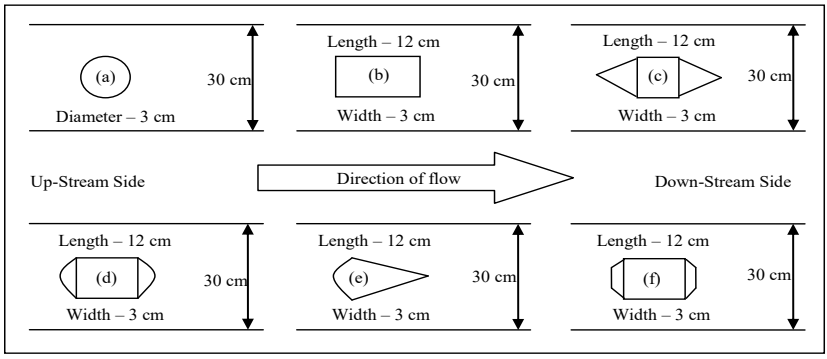

Figure 5: Different form of pier namely, (a) circular, (b) rectangular, (c) sharp-nosed, (d) oblong, (e) joukowsky, and, (f) chamfered

Figure 5 illustrates the various diameters and shapes of six-bridge piers, namely circular, rectangular, sharp-nosed, oblong, joukowsky and chamfered, as seen inside the rectangular flume. Based on the research conducted by Tafarojnoruz et al (2010), it is advised that the cross section should be limited to a maximum of 10% of the flume width. This limitation is crucial in mitigating the wall effect phenomenon that might potentially lead to scouring. The width of the pier in this study conforms to the parameters outlined by Vijayasree and Eldho (2016), as it is kept at a ratio of 10% to the width of the flume.

Sediment Analysis

A physical sieve analysis test is conducted to establish the particle size which utilized inside the flume. The findings of the study indicate that the average particle size (d50) measures 0.39 mm, while the standard deviation of the bed material (β) i.e.

$\left(\beta = \left(\frac{d_{84}}{d_{16}}\right)^{0.5}\right)$ is 1.33. The incorporation of the pier's diameter is a crucial factor to take into account while neglecting the impact of particle size on depth of the scour. According to the research conducted by Nabil et al (2022), it is evident that the influence of grain size on scouring depth diminishes in significance when the ratio of the width of the pier to the grain size (b/d50) exceeds around 25. The empirical findings suggest that a pier diameter of 30.0mm yields a ratio of around 76.92, aligning with the suggestions given by Nabil et al. (2022). Following each experimental trial, the bed materials inside the flume is meticulously dressed and leveled with the use of a scraping tool. This measure is implemented with the purpose of mitigating the formation of ripples and dunes, as seen in figures 6(a)–(d).

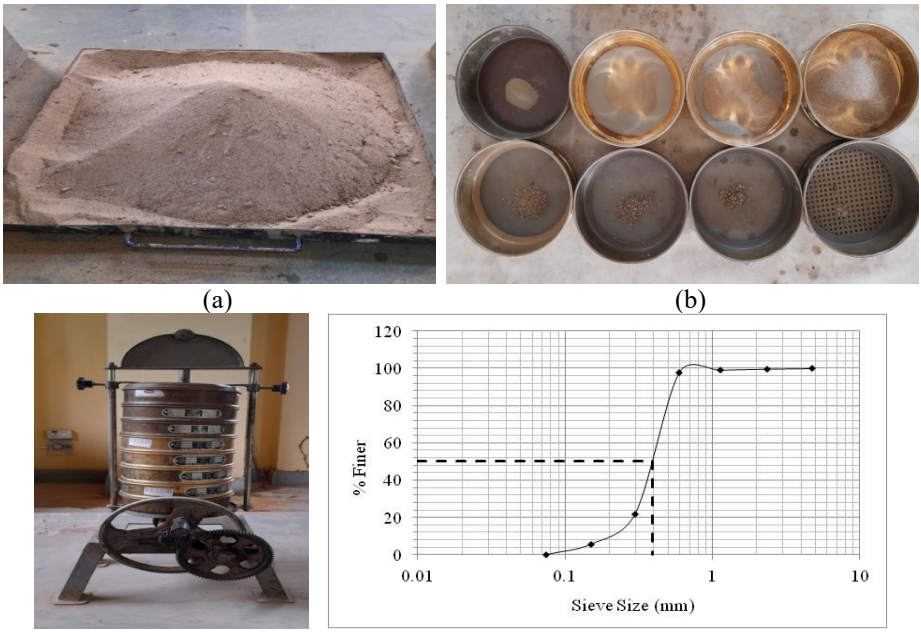

Figure 6(a)–(d): Details of sediment analysis of bed materials including particle sieve analysis graph

In the present study, the ratio between the width of the pier and the mean size of sediment (b/d_{50}) was found to be 76.92, suggesting that the sediment may be categorized as coarse sand. In their study, Yang et al. (2018) established a classification system for the diameter of bridge piers, taking into account the features of sediment size. They particularly identified a threshold of b/d_{50} above 130 for this classification.

Technique for experimentation

The tests were conducted on a steady subcritical flow, where the velocity (V) was less than or equal to the critical velocity (V_c) and the Froude number (F_r) was less than 1. These examinations were conducted under the circumstances of clear water scour (CWS), specifically focusing on the plain bed configuration. It was important to prevent the development of ripples and dunes in the upstream part of the working section. Using a wooden flat surface, the flume's bed is leveled. The vertical placement of bridge piers of various forms inside the central portion of the flume is followed by the subsequent leveling of the bed surface. In order to mitigate disruption and minimize the jerk impact on the bed sediment caused by the abrupt increase in water velocity, the pump was halted after an initial duration of 120 seconds. During this temporal interval, the flume is inundated with water through the pump's hose, while the bed sediment is afterwards smoothed by manual means to prevent the formation of undulations and sand hills. Following a brief interval, the pump recommenced operation once the flow level reached a state of equilibrium, with the measurement of flow depth being conducted using a point gauge. The experimental run is expected to last for a length of 300 minutes. According to Eldho et al. (2010), it has been noted that the displacement of silt near the bridge piers slows down significantly after a certain period of time. As stated by Setia (2008), the attainment of equilibrium in the scour hole surrounding a bridge pier imposes limitations on the extent of quantitative investigation, since it is confined to the maximum depth of scour achievable. The velocity of water flow through the flume is intentionally reduced to mitigate any disturbances in the scour hole, so facilitating the desiccation of silt. Following that, the depth of scour is assessed in the area of the pier. In instances involving pier models of varying shapes, the method of leveling the bed surface of the flume is reiterated in accordance with the aforementioned protocols.

Test program

To prevent the bridge from failing, scour depth calculations are made using a test program to calculate the pier's various configurations. Experimental results are compared with the observed depth of scour near six distinct shapes, namely circular, rectangular, sharp-nosed, oblong, joukowsky and chamfered piers. The maximum depth of scours near each of the six bridge pier models is calculated using a range of discharge rates (from 0.00104 cumecs to 0.00157 cumecs) when the ratio of actual velocity (V) and critical velocity (Vc) is less than one under the CWS condition, with no angle of attack i.e., $\left(\left(\frac{V}{V_c}\right) \leq 1\right)$ (Lança et al., 2013). The equation (1) proposed by Fael et al. (2016) is used to determine the critical velocity. Table 2 displays the testing conditions for all six bridge pier configurations.

Table 2 presents the variables used in this study, where the symbol b represents the pier width in meters, y denotes the flow depth in meters, Q represents the water discharge in cubic meters per second, V represents the flow velocity in meters per second, V_c

represents the critical velocity of flow in meters per second, V/Vc represents the non-dimensional velocity ratio, and Fr denotes the Froude number.

HEC-RAS Analysis

The HEC-RAS program is utilized to evaluate the occurrence of scour in the proximity of bridge piers. The subsequent model is a one-dimensional simulation that effectively depicts sediment transport in situations including moveable boundaries, encompassing both steady and turbulent flow conditions. To get further details, readers are advised to refer to the HEC-RAS manual 6.2. Mehta et al. (2020) developed a stable channel using the HEC-RAS software for the Surat region. The findings suggest that the model effectively forecasts the morphology and key measurements of stable channels in rivers. In order to effectively utilize HEC-RAS, it is important to have both geometry and flow data pertaining to the river. The dataset pertaining to the geometry comprises many cross-sectional profiles situated both in the upstream and downstream regions of the bridge. The cross-sectional profiles are strategically positioned at regular intervals, serving as valuable sources of data about the roughness coefficient of both the river and flood plain. Conversely, the flow data includes discharge values that correspond to different return times. Figure 7 illustrates a sequential approach for the creation of the model in the form of a bar chart.

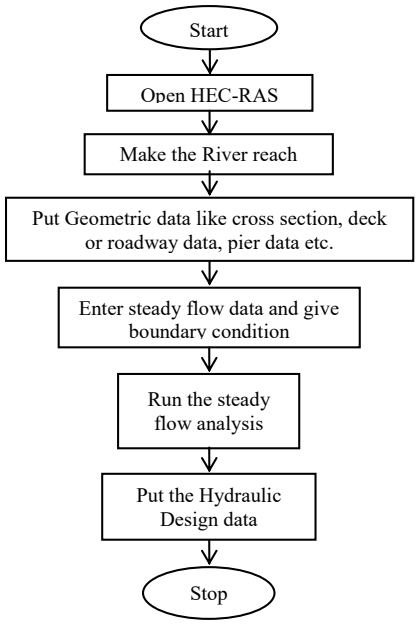

Figure 7: Bar chart for the creation of the model

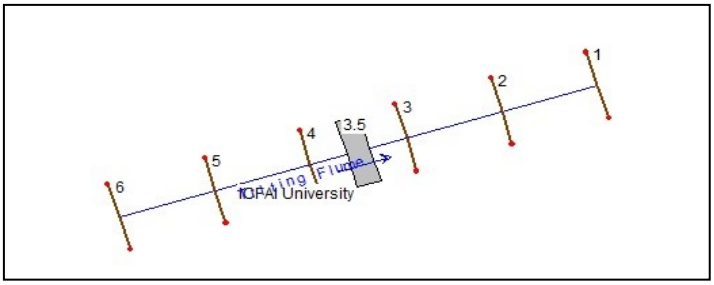

Figure 8: Cross-sections of the Tilting flumes plotted in the HEC-RAS modeling tool

In this present study a model is prepared using HEC-RAS modeling tool to estimate scour around bridge pier. Different pier shapes are used to see the variation on scour depth. The data which have used in the experimental procedure are also used to develop the model in HEC-RAS to establish a correlation between them. The geometric profile of model is shown in the figure 8

RESULTS AND ANALYSIS

The tests include adjusting of various hydraulic factors on six distinct bridge pier designs, namely circular, rectangular, sharp-nosed, oblong, joukowsky and chamfered. The measurement of depth of local scour is conducted at the upstream side of the bridge pier's tip for all six forms.

Changes in depth of scour with flow rate

The studies performed in Table 3 assessed the depth of scour (y_s) near all piers of various forms, using discharge ranging from 0.00104 cumecs to 0.00157 cumecs. Percentage increments in depth of scour associated with the increment in discharge for different shapes of pier are provided in Table 3. The reference discharge of 0.00104 cumecs was used as a baseline, and further measurements were taken after increasing the velocity by about 16%, 29%, and 51%. The corresponding scour depth was then recorded. The experimental findings are shown in Figures 9(a)–(b). The relationship between the increase in discharge and the depth of local scour for various shapes of bridge piers, namely circular, rectangular, sharp-nosed, oblong, joukowsky and chamfered is provided in Table 4. On the other hand, Table 5 illustrates the variation in discharge increase as a percentage with regard to the depth of local scour for the same shapes of bridge piers.

Based on the analysis of Figure 9(a), it can be seen that there is a significant augmentation in the depth of local scour when the discharge varies from 0.00104 cumecs to 0.00157 cumecs. When tested separately and at a particular discharge, the rectangular shape of the bridge pier exhibits the greatest depth of scour. Conversely, the sharp-nosed shape of the bridge pier exhibits the least depth of local scour. The local scour depth of the remaining forms of bridge piers, in decreasing order, is as follows: round, chamfered, Joukowsky, and rectangular shapes. In Figure 9(a), it is seen that an increase in discharge results in a

corresponding rise in scour depth around all six piers of varying forms. Notably, the rectangular pier shape exhibits the highest recorded scouring, while the sharp-nosed pier shape exhibits the least recorded scouring.

Figure 9(b) depicts the correlation between the rise in depth of scour and the rise in discharge percentage for all the different forms of piers. The analysis of Figure 9(b) reveals that, out of the six designs under investigation, the oblong configuration of the bridge pier exhibits the most advantageous characteristics. This can be attributable to the relatively smaller percentage rise in the depth of scour. On the other hand, the circular form of the bridge pier exhibits the least desirable attributes, as it demonstrates a higher percentage increase in the depth of scour. The remaining shapes, namely chamfered, rectangular, sharp nose, and joukowsky, display varying degrees of scour depth increase, with the oblong shape falling between the circular and sharp nose shapes in terms of decreasing order.

Table 2: Experimental results for six different pier shapes

Sl. no	Pier nose shape	Breadth (m)	Water Depth (m)	Discharge (cumecs)	Velocity (m/s)	V/V_c	F_r
1	Circular	0.03	0.151	0.00104	0.23	0.068	0.189
2		0.03	0.155	0.00121	0.26	0.076	0.211
3		0.03	0.159	0.00134	0.28	0.082	0.225
4		0.03	0.164	0.00157	0.32	0.093	0.252
5	Rectangular	0.03	0.155	0.00104	0.22	0.066	0.181
6		0.03	0.157	0.00121	0.26	0.075	0.207
7		0.03	0.164	0.00134	0.27	0.079	0.215
8		0.03	0.170	0.00157	0.31	0.089	0.238
9	Sharp-nosed	0.03	0.145	0.00104	0.24	0.071	0.200
10		0.03	0.149	0.00121	0.27	0.080	0.224
11		0.03	0.153	0.00134	0.29	0.086	0.238
12		0.03	0.161	0.00157	0.33	0.095	0.259
13	Oblong	0.03	0.148	0.00104	0.23	0.069	0.194
14		0.03	0.151	0.00121	0.27	0.079	0.219
15		0.03	0.157	0.00134	0.28	0.083	0.229
16		0.03	0.163	0.00157	0.32	0.093	0.254
17	Joukowsky	0.03	0.150	0.00104	0.23	0.068	0.191
18		0.03	0.155	0.00121	0.26	0.076	0.211
19		0.03	0.161	0.00134	0.28	0.081	0.221
20		0.03	0.166	0.00157	0.32	0.092	0.247
21	Chamfered	0.03	0.150	0.00104	0.23	0.068	0.191
22		0.03	0.154	0.00121	0.26	0.077	0.213
23		0.03	0.160	0.00134	0.28	0.082	0.223
24		0.03	0.167	0.00157	0.31	0.091	0.245

Variation of scour depth with depth of flow, velocity of flow and Froude number

The non-dimensional depth of scour (y_s/b) is determined for piers of various forms, and the corresponding measurements are depicted in figures 10(a)–(c). The maximum discharge of 0.00157 cumecs is used to calculate the non-dimensional flow discharge (Q/Q_{max})

Figure 10(a) illustrates the correlation between the depth of scour (y_s/b) and the stream discharges. The rectangular pier exhibits a greater range of depth scour variations compared to the sharp-nosed design when the discharge rises from 0.66 to 1.0. Nevertheless, it is crucial to acknowledge that the augmentation in scour depth does not exhibit a linear pattern throughout all six configurations.

Table 3: An overview of the dimensionless scour depth measurements for different pier shapes

Sl. No	Pier nose shape	*Q (m^3/s)*	*V/V_c*	*$y_{s/b}$*	*y_s (m)*
1	Circular	0.00104 - 0.00157	0.068 – 0.093	1.07 – 1.53	0.032- 0.046
2	Rectangular	0.00104 - 0.00157	0.066 – 0.089	1.27 – 1.80	0.038 – 0.054
3	Sharp - nosed	0.00104 - 0.00157	0.066 – 0.095	0.87 – 1.07	0.026 – 0.032
4	Oblong	0.00104 - 0.00157	0.069 – 0.093	1.03 – 1.13	0.031 – 0.034
5	Joukowsky	0.00104 - 0.00157	0.076 – 0.092	0.030 – 0.036	
6	Chamfered	0.00104 - 0.00157	0.068 – 0.091	0.031 – 0.042	

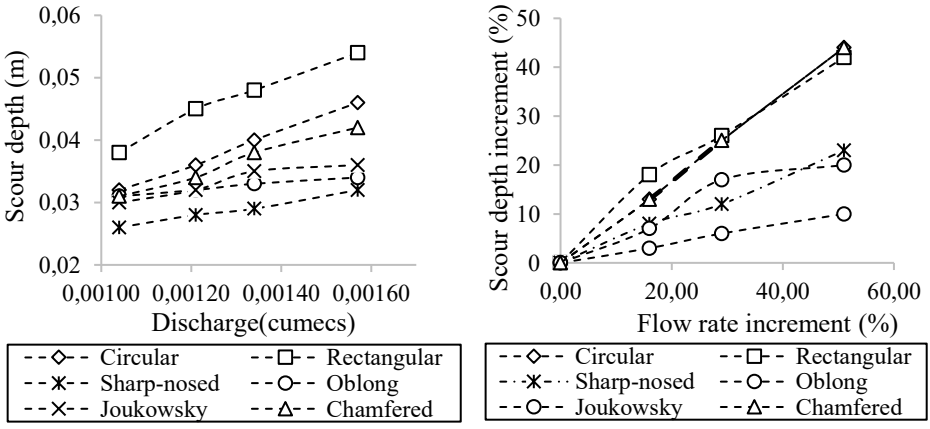

(a) (b)

Figure 9: Changes in (a) pier shapes and depth of scour (y_s) at discharges ranging from 0.00104 to 0.00157 cumecs and (b) percentage increment in depth of scour with percentage increment in discharge

As shown in Figure 10(b), the non-dimensional depth of scour (y_s/b) near the rectangular pier increases from 1.27 to 1.80 as the non-dimensional depth of flow (y/b) rises from 5.17 to 5.67. Among the six unique pier designs studied, this is the deepest scour that was discovered. The sharp-nosed pier, on the other hand, has the shallowest non-dimensional depth of scour (y_s/b) in the vicinity of any of the pier types studied. It's vital to remember that the depth of scour does not rise at a constant rate. The Froude Number is a dimensionless parameter that quantifies the ratio of inertial forces to gravitational forces. When the Froude Number is less than 1, the flow is classified as subcritical, indicating that gravity forces dominate over viscous forces. This condition of flow is sometimes referred to as sluggish and calm. When the value exceeds 1, indicating that viscous forces surpass gravity forces, the flow is referred to as a supercritical flow, which is alternatively described as a condition of fast and rapid flow. As the Froude's number grows, there is a corresponding increase in the velocity of flow, leading to an increase in the depth of scour. Figure 10(c) shows that for six different forms, the non-dimensional depth of scour (y_s/b) grows as the Froude number (F_r) increases. It should be stressed, however, that this growth is not linear. There was an initial increase from 0.130 to 0.151 in the Froude number (F_r), which was mirrored by a rise in the depth of scour of the piers from 0.67 to 1.10. Non-dimensional depth of scour is relatively constant in size. Non-dimensional depth of scour measurements showed an array of 0.75 to 1.53 when the Froude number was raised from 0.148 to 0.218, suggesting a considerable increase.

Table 4: Changes in the increase in rate of flow with depth of local scour for different pier shapes

Pier nose shape	**Flow rate increment (m^3/s)**			
	0.00104	0.00157	0.00134	0.00157
	Local Scour depth (m)			
Circular	0.032	0.036	0.040	0.046
Rectangular	0.038	0.045	0.048	0.054
Sharp - nosed	0.026	0.028	0.029	0.032
Oblong	0.031	0.032	0.033	0.034
Joukowsky	0.030	0.032	0.035	0.036
Chamfered	0.031	0.034	0.038	0.042

Table 5: Changes in the augmentation of flow rate with local scour depth

Pier nose shape	**Increment in flow rate (%)**			
	0	16	29	51
	Increment in depth of local scour (%)			
Circular	0	13	25	44
Rectangular	0	18	26	42
Sharp - nosed	0	8	12	23
Oblong	0	3	6	10
Joukowsky	0	7	17	20

Chamfered	0	13	25	44

When the experiment is over, the bed material is efficiently flushed away thanks to the flow around the pier models. A point gauge positioned on the upstream face of the pier nose is used to measure the depth of scour in the immediate area. Each of the six different kinds of bridge piers will have its scouring pattern and depth of scour measured throughout the testing process. By referring to Figures 11(a)-(f), the maximum depth of scour may be calculated. Scour hole diameters vary over the length of different bridge pier types, as seen in Figure 10. Figure 11(a) shows how the scour hole pattern is much narrower on the downstream side of the rectangular bridge pier than on the upstream side. Figures 11(c)–(f) show that the aforementioned pattern also appears in the joukowsky, chamfered, sharp-nosed, and rectangular bridge pier designs. Figure 11(b) shows that the scour holes are dispersed in a manner that is consistent and equally spaced throughout the bridge pier's circular shape.

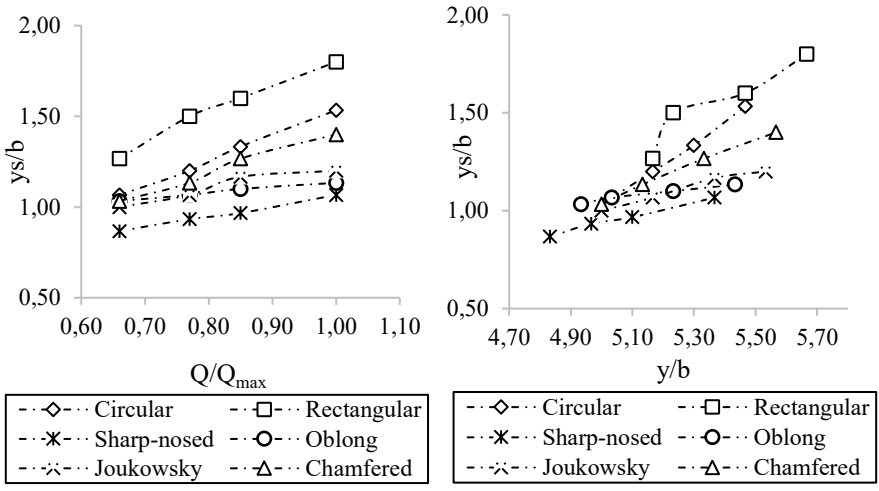

(a) (b)

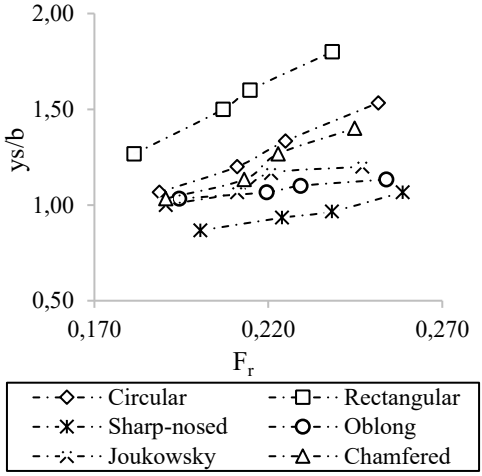

(c)

Figure 10: Variations of the non-dimensional depth of local scour (ys/b) for piers of six various forms with (a) the non-dimensional rate of flow (Q/Q_{max}), (b) the non-dimensional flow depth (y/b), and (c) the Froude number (F_r)

Comparison of the current work with CSU (1975), the scour depth prediction equation developed by Breusers et al. (1977), and the HEC-RAS modeling tool

The HEC-18 equation, which was derived by the US Department of Transportation's Federal Highway Administration (FHWA), was established via the analysis of laboratory data pertaining to the cylindrical configuration of bridge piers. The proposed improvements include making changes to the width of the pier, adjusting the size of the bed material, and taking into account the many aspects that contribute to the effect of bed forms (Richardson et al. 2001). In order to augment the wide range of the data evaluation in this study, the researchers used the equilibrium depth of scour estimation equations developed by the University of Colorado (CSU) in 1975. The equations indicated above were used to assess the current findings and ascertain the anticipated equilibrium depth of scour for the specific experimental circumstances linked to each pier configuration. The present work used the CSU (1975) equation, a widely used equation for predicting equilibrium depth of scour, to compute the non-dimensional depth of scour based on the collected data. In this methodology, careful examination is conducted on each individual form. The aim of this study is to find the efficacy of the CSU (1975) equation, a well-recognized equation used for predicting the depth of scour that has been thoroughly examined in the existing scholarly discourse. The equation denoted as (3) in the CSU (1975) study is presented.

$$\frac{y_{se}}{b} = 2K_1K_2K_3K_4\left(\frac{y}{b}\right)^{0.35} F_r^{0.43} \quad (3)$$

The equilibrium scour depth, often represented as y_{se}, is subject to the effects of several variables. The coefficient of correction K_1 denotes the impact of pier morphology, especially the ratio between the length and breadth of the pier. In the context of a circular pier, it may be said that the value of K_1 is equivalent to 1. The correction factor K_2 is used to compensate the effect of attack angle of flow. In the context of a conventional approach flow, the value of K_2 is equivalent to 1. The correction factor K_3 accounts for the influence of bed shape on the flow. In the context of a scenario with a flatbed subjected to clear water scour (CWS), the value of K_3 is determined to be 1. The last element, denoted as K_4, pertains to the consideration of sediment mixes and their impact. When the sediment demonstrates homogeneity, the numerical value of K_4 is equal to 1. The equation, first introduced by CSU in 1975, has gained recognition and use due to its applicability to various bridge pier forms in clear water scenarios.

$$y_{se} = 2K_1 y^{0.35} b^{0.65} F_r^{0.43} \quad (4)$$

The modification of the configuration of a bridge pier, denoted as K_1, is commonly referred to as the shape factor, denoted as K_{sh}. The use of K_{sh} has been suggested in several studies as a means to achieve uniform pier shape, wherein piers keep a consistent cross-sectional area over their whole depth. The researchers encompassed in this study are Tison et al (1940), Guan et al (2022), Laursen et al (1956), Fakhimjoo et al (2023), Novak et al (2017), Pizarro et al (2020), and Jan et al (2022). The form factor may be characterized as the ratio between the depth of scour recorded for a non-circular pier and the depth of scour estimated for a circular pier, as stated by Kassem et al. (2023). The formula used by Rafiqui et al. (2023) is provided in equation (5).

$$K_{sh} = \frac{y_{se}(non-circular)}{y_{se}(Circular)} \quad (5)$$

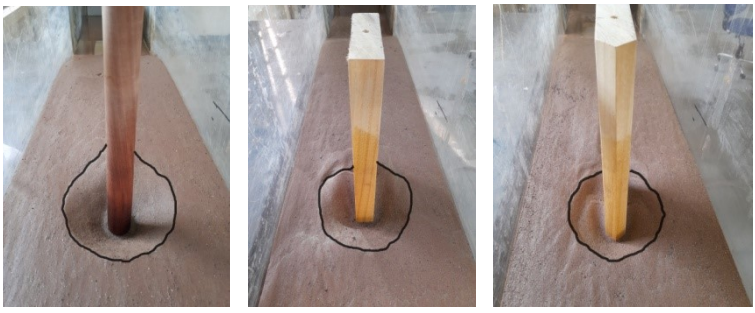

(a) (b) (c)

(d) (e) (f)

Figure 11: Scouring pattern at the upstream front of (a) circular, (b) rectangular, (c) sharp-nosed, (d) oblong, (e) joukowsky, and (f) chamfered piers during trial run

For non-circular piers, we have y_{se} (non-circular) which represents the equilibrium depth of scour, while on circular piers, we have y_{se} (circular), which represents the equilibrium depth of scour.

In the experimental investigation conducted by Rafiqui et al. (2023), it was shown that the impact of the form factor is only noticeable when the flows are exposed to a zero-degree angle of attack. The equation that Breusers et al (1977) gave is shown in equation (6).

$$y_{se} = 1.35 K_1 y^{0.30} b^{0.70} \tag{6}$$

The shape factor, denoted as K_1, is a variable. It is dependent on the ratio of pier length to width, referred to as the pier, and is influenced by the flow depth (y) and pier width (b).

Table 6: detailed comparison of CSU (1975), HEC-RAS modeling tool, and Breusers et al. (1977)

Sl. No.	Shape of pier nose	K_1	(Q/Q_{max})	Non-dimensional scour depth (y_s/b)			
				Present Study	HEC-RAS	CSU (1975)	Breusers et al (1977)
1	Circular	1.0	0.66	1.07	1.52	1.72	2.19
2			0.77	1.20	1.62	1.82	2.21
3			0.85	1.33	1.69	1.89	2.23
4			1.00	1.53	1.80	2.00	2.25
5	Rectangular	1.082	0.66	1.27	1.65	1.85	2.39
6			0.77	1.50	1.76	1.96	2.40
7			0.85	1.60	1.82	2.02	2.43
8			1.00	1.80	1.94	2.14	2.46

9	Sharp-nosed	0.706	0.66	0.87	1.03	1.23	1.53
10			0.77	0.93	1.10	1.30	1.54
11			0.85	0.97	1.15	1.35	1.55
12			1.00	1.07	1.22	1.42	1.58
13	Oblong	0.764	0.66	1.03	Shape	1.32	1.66
14			0.77	1.07	not	1.40	1.67
15			0.85	1.10	available	1.45	1.69
16			1.00	1.13		1.53	1.71
17	Joukowsky	0.882	0.66	1.00	Shape	1.52	1.93
18			0.77	1.07	not	1.61	1.95
19			0.85	1.17	available	1.66	1.97
20			1.00	1.20		1.76	1.99
21	Chamfered	0.964	0.66	1.03		1.66	2.11
22			0.77	1.13	Shape	1.76	2.13
23			0.85	1.27	not	1.82	2.15
24			1.00	1.40	available	1.92	2.18

Table 6 presents a comparative study of the current research findings and the experimental results obtained using the CSU (1975), the HEC-RAS modeling tool and Breusers et al (1977). The determination of the local scour depth is conducted for each of the six categories of piers, specifically round, rectangular, sharp-nosed, oblong, joukowsky, and chamfered. The prediction equation for scour depth, as provided by CSU (1975), HEC-RAS modeling tool, and Breusers et al. (1977), was employed to ascertain the unique curves for each of the piers, as seen in figures 13(a - f).

Figure 12 illustrates the variation between predicted and observed scour depths. Prediction of scour depth is accomplished using the CSU equation (1955), the HEC-RAS modeling tool and the Breusers et al. (1977) equation. These values are compared with the measured scour depth that was acquired from the experiment in tilting flume. A best-fitted line is formed to identify the most reliable instrument for estimating the depth of scour. From the graph, it is easily observed that the scour depth obtained by the HEC-RAS modeling tool is closer to the best fitted line compared to other equations.

Figure 13(a) illustrates a consistent and upward trend in the curve, and the variations seen in the curve may be attributed to the experimental circumstances. Figure 13(b) exhibits a comparable and ascending trend in the curve, and the dissimilarity in the curve may be elucidated by considering the experimental circumstances, which are identical to those in Figure 13(a).

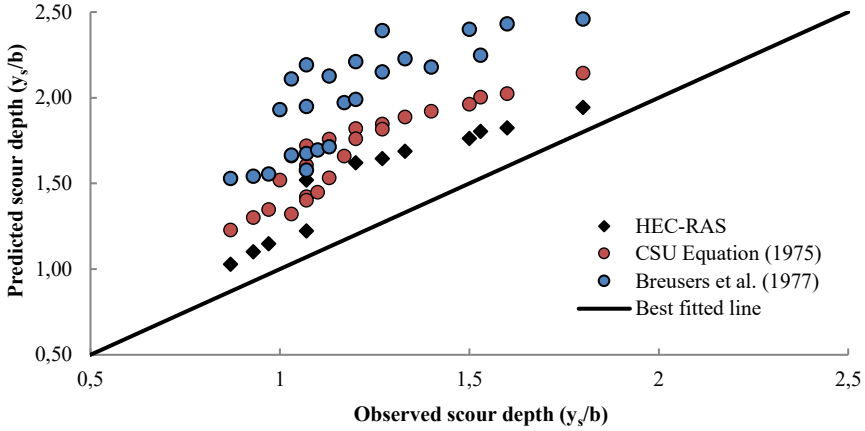

Figure 12: Comparison between observed scour depth and predicted scour depth

To facilitate a comparison between the outcomes of this research and the depth of scour prediction equations proposed by Breusers et al. (1977) and CSU (1975), Figure 13(c) presents a dimensionless analysis of the depth of scour. By incorporating data obtained from all three sources, a unified equation for the depth of scour is derived. Figures 13(d)–(f) illustrate a dimensionless examination of the outcomes obtained from the scour depth prediction equation proposed by CSU (1975), Breusers et al. (1977), and the current investigation. The figures provided enable a comparison between the equations given before and enable the formulation of a full depth of scour equation that incorporates all three datasets.

DISCUSSION

A thorough analysis of the conical morphology reveals that the region of maximum depth is situated in the downstream vicinity of the bridge piers. The soil characteristics of the channel beds also have an impact on the depth of the scour hole in proximity to bridge piers. It is essential to acknowledge that the kind of vortex that develops near bridge piers has an influence on the scouring phenomenon occurring in that vicinity. The scouring operation is influenced by several elements, such as the shape of the pier and the velocity of the water.

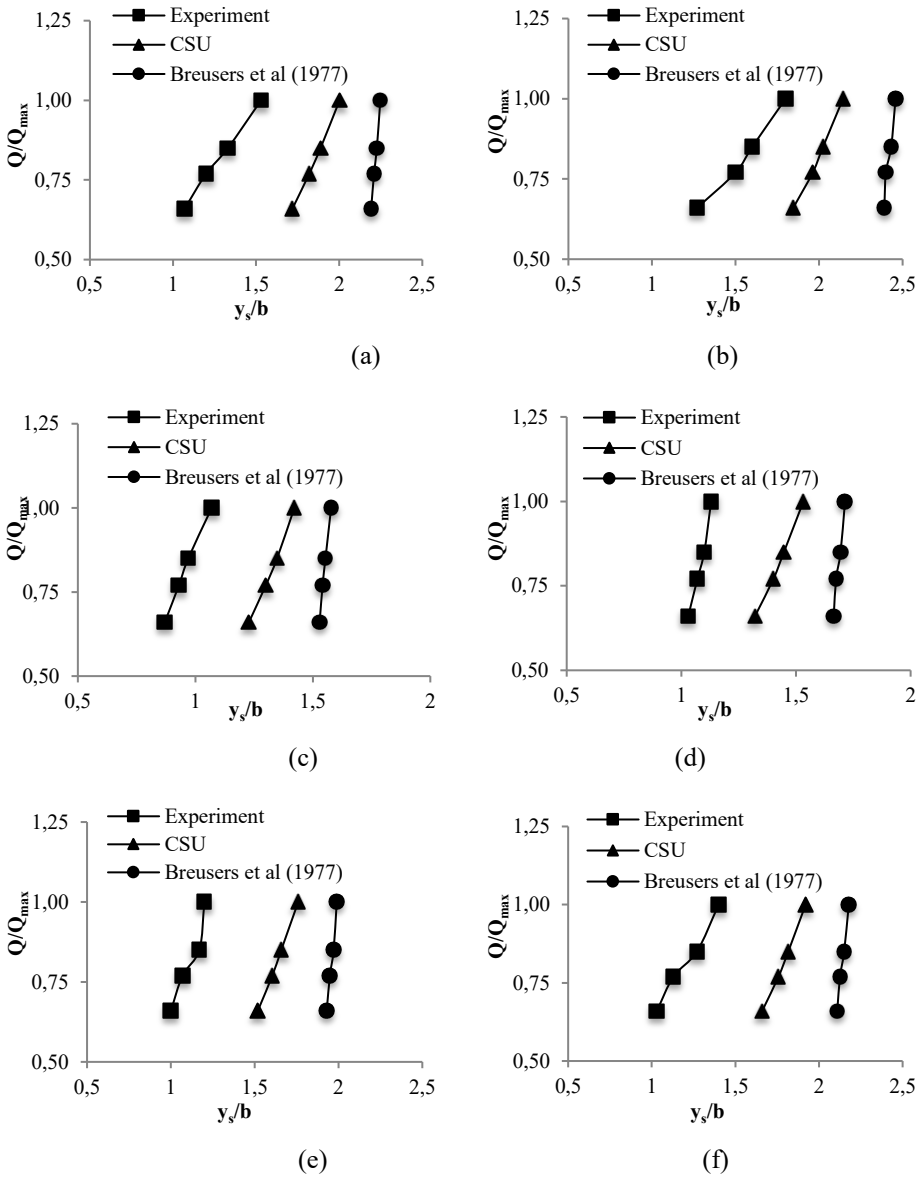

Figure 13: Comparison of non-dimensional depth of scour (y_s/b) with non-dimensional rate of flow (Q/Q_{max}) for (a) circular, (b) rectangular, (c) sharp-nosed, (d) oblong, (e) joukowsky, and, (f) chamfered pier

Notably, scouring tends to be more pronounced on the upstream side of the pier, while being comparatively less significant on the downstream side. The findings indicate that the depth of local scour around a rectangular-shaped bridge pier is measured at 8.0 cm, which can be attributed to its bigger frontal exposure. In contrast, it has been observed that the typical scour level near a bridge pier in a sharp nose configuration measures 5.3 cm, a phenomenon that may be related to the reduced frontal blocked area of the pier. The results of the study suggest that the rectangular bridge pier experiences the highest depth of scour at different flow velocities, while the sharp-nosed bridge pier has the lowest depth of scour. The present study involved a comparative analysis of the acquired results using the equations put out by Breusers et al (1977), CSU (1975) and HEC-RAS modeling tool in order to estimate scour depth. Furthermore, a comprehensive analysis was undertaken to examine the fundamental mechanism of scour, utilizing the dataset acquired in the present investigation. The research demonstrates that the curve has a continuous and upward direction, indicating a discernible pattern of expansion. The observed fluctuations in the curve can be attributed to the particular experimental conditions employed. The results suggest that there is a positive correlation between depth of scour and rate of flow, and the observed pattern in the graph is consistent with the formulas presented by the CSU (1975), the HEC-RAS modeling tool, and the Breusers et al (1977). The findings presented in this study offer substantiation for the reliability of the experimental methodologies implemented. The experiments conducted on all six bridge pier forms yielded a range of discharge and velocity values. Specifically, the observed range of discharge varied from 0.00104 cumecs to 0.00157 cumecs, while the range of velocity ranged from 0.22 m/s to 0.33 m/s. The present hydraulic circumstances differ from the projected depth of scour conditions suggested by CSU (1975) and Breusers et al (1977), perhaps accounting for the observed lower values of y_s/b in comparison to the predictions made by CSU (1975) and Breusers et al (1977).

CONCLUSION

This research encompasses the conduct of tests involving various hydraulic factors. A series of six bridge piers, each possessing distinct forms including circular, rectangular, sharp-nosed, oblong, joukowsky and chamfered, were constructed for the purpose of evaluating scour depth and examining the resulting scour pattern. These investigations were conducted via meticulous experimental examinations.

The current investigation may be briefly summarized as follows.

It has been found that scour holes formed in non-cohesive materials have a conical shape, with the greatest depth occurring at the snout of the bridge piers in the upstream direction.

The rectangular pier has shown the highest scour depth at a certain velocity, making it the least favorable shape in this study. Conversely, the sharp-nosed pier has shown to have the lowest scour depth owing to its lower frontal exposed area, making it the most favorable form within the scope of these trials.

The current investigation was a comparison of the depth of scour estimation equations proposed by CSU (1975) and Breusers et al (1977). A direct correlation between the depth of scour and the velocity of the flow was noted. Moreover, the observed trend depicted in the graph had a strong resemblance to the equations put forward by Breusers et al (1977) and CSU (1975), hence providing validation for the experimental findings.

The HEC-RAS modeling tool is capable of accurately predicting the level of scour depth, making it the most appropriate instrument for computing scour depth.

The scour hole pattern seen in circular bridge piers has a near-uniform distribution across the structure.

The geometric arrangement of a pier has a crucial influence on the occurrence of scouring. The erosive phenomena seen in the area of the individual pier were predominantly influenced by the geometric attributes of the bridge pier. The geometric parameters of the pier shape were seen to have an impact on both the position and extent of the maximum depth of scour. The current investigation has yielded the observation that the scour depth is minimized when employing a pier with a sharp nose shape. Hence, if this outcome is integrated prior to the design of the bridge pier, it would effectively guarantee both the safety and serviceability of the bridge.

Declaration of competing interest

The authors declare that they have no known competing financial interests or personal relationships that could have appeared to influence the work reported in this paper.

REFERENCES

ABUDALLAH HABIB, I., WAN MOHTAR, W. H. M., MUFTAH SHAHOT, K., EL-SHAFIE, A., ABD MANAN, T. S. (2021). Bridge failure prevention: An overview of self-protected pier as flow altering countermeasures for scour protection, Civil Engineering Infrastructures Journal, Vol. 54, Issue 1, pp. 1-22.

ACHOUR B., AMARA L., MEHTA D. (2022). Control of the hydraulic jump by a thin-crested sill in a rectangular channel new experimental considerations, Larhyss Journal, No 50, pp. 31-48.

ACHOUR B., AMARA L., MEHTA D., BALAGANESAN P. (2022). Compactness of Hydraulic Jump Rectangular Stilling Basins Using a Broad-Crested Sill, Larhyss Journal, No 51, pp. 31-41.

ACHOUR B., AMARA L., MEHTA D. (2022). New theoretical considerations on the gradually varied flow in a triangular channel, Larhyss Journal, No 50, pp. 7-29.

ADIB A., TABATABAEE S. H., KHADEMALRASOUL A., SHOUSHTARI M. M. (2020). Recognizing of the best different artificial intelligence method for determination of local scour depth around group piers in equilibrium time, Arabian Journal of Geosciences, Vol. 13, pp. 1-11.

AL-SHUKUR A. H. K., OBEID Z. H. (2016). Experimental study of bridge pier shape to minimize local scour, International Journal of Civil Engineering and Technology, Vol. 7, Issue 1, pp. 162-171.

BIAN R., TOLFORD T. (2023). Evaluating the implementation of the complete streets policy in Louisiana: a review of practices and projects in the last 10 years, Transportation research record, Vol. 2677, Issue 3, pp. 505-520.

BOR A. S. L. I., GUNEY M. Ş. (2022). Experimental and numerical investigation of local scour around square bridge pier, J. Eng. Sci. Technol., Vol. 17, pp. 404-0419.

BREUSERS H. N. C., NICOLLET G., SHEN H. W. (1977). Local scour around cylindrical piers. Journal of hydraulic research, Vol. 15, Issue 3, pp. 211-252.

BREUSERS H. N. C. (2020). Scour around spur dikes and abutments. In Scouring, CRC Press, pp. 51-59.

CHAVAN V. S. (2021). Finite Element Modeling of a Pier-on-Bank Bridge Scour (Doctoral dissertation, The University of North Carolina at Charlotte).

CHIEW Y. M. (1984). Local scour at bridge piers (Doctoral dissertation, ResearchSpace@ Auckland).

CHOI S. U., CHOI S., CHOI B. (2021). Prediction of time dependent local scour around bridge piers in non-cohesive and cohesive beds using machine learning technique, Journal of Korea Water Resources Association, Vol. 54, Issue 12, pp. 1275-1284.

CHOOPLOU C. A., VAGHEFI M., AKBARI M. (2023). Effect of repositioned submerged vanes on local scour variations around a pier in a bend: experimental investigation, International Journal of Environmental Science and Technology, pp. 1-14.

DOU X. (1997). Numerical simulation of three-dimensional flow field and local scour at bridge crossings. The University of Mississippi.

EBRAHIMI M., KRIPAKARAN P., PRODANOVIĆ D. M., KAHRAMAN R., RIELLA M., TABOR G., DJORDJEVIĆ S. (2018). Experimental study on scour at a sharp-nose bridge pier with debris blockage, Journal of Hydraulic Engineering, Vol. 144, Issue 12, pp. 04018071.

ELDHO T. I., VISWANADHAM B. V. S., VIJAYASREE B. A. (2010). Physical model study of scouring effects on pier foundations of bridges, In Proceedings of Indian Geotechnical Conference 2010, GEOtrendz, pp. 16-18.

ESCAURIAZA C., GONZÁLEZ C., WILLIAMS M. E., BREVIS W. (2023). Models of bed-load transport across scales: turbulence signature from grain motion to sediment flux. Stochastic Environmental Research and Risk Assessment, Vol. 37, Issue 3, pp. 1039-1052.

ETTEMA R., NAKATO T., MUSTE M. V. I. (2006). An illustrated guide for monitoring and protecting bridge waterways against scour (No. Project TR-515). IIHR-Hydroscience & Engineering, University of Iowa.

FAEL C., LANÇA R., CARDOSO A. (2016). Effect of pier shape and pier alignment on the equilibrium scour depth at single piers, International Journal of Sediment Research, Vol. 31, Issue 3, pp. 244-250.

FAKHIMJOO M. S., ARDESHIR A., BEHZADIAN K., KARAMI H. (2023). Experimental investigation and flow analysis of clear-water scour around pier and abutment in proximity, Water Science and Engineering, Vol. 16, Issue 1, pp. 94-105.

FLEIT G., BARANYA S., EHLERS R., BIHS H. (2023). CFD modeling of flow and local scour around submerged bridge decks. Journal of Coastal and Hydraulic Structures, 3.

GHASEMI ASL M., HEIDARNEJAD M. (2023). A numerical study of the maximum scour depth around inclined bridge piers and comparison with an experimental model, Larhyss Journal, No 56, pp. 55-75.

GUAN D. W., XIE Y. X., YAO Z. S., CHIEW Y. M., ZHANG J. S., ZHENG J. H. (2022). Local scour at offshore windfarm monopile foundations: A review, Water Science and Engineering, Vol. 15, Issue 1, pp. 29-39.

HARASTI A., GILJA G., POTOČKI K., LACKO M. (2021). Scour at bridge piers protected by the riprap sloping structure: A review, Water, Vol. 13, Issue 24, pp. 3606.

HELMY A., ALI M., AHMED H. (2017). An experimental study of local scour around piers in the curved channels. Journal of Multidisciplinary Engineering Science and Technology, Vol. 4, Issue1, pp. 6448-6453.

JAN R., LONE M. A. (2022). Effect of mutual interference of piers on their local scour phenomenon. Innovative Infrastructure Solutions, Vol. 7, Issue 2, pp. 186.

JALAL H. K., HASSAN W. H. (2020). Effect of bridge pier shape on depth of scour. In IOP conference series: materials science and engineering, Vol. 671, No. 1, p. 012001). IOP Publishing.

JIA J., JI A. (2018). Soil dynamics and foundation modeling, New York: Springer.

JUEYI S. U. I., AFZALIMEHR H., SAMANI A. K., MAHERANI M. (2010). Clear-water scour around semi-elliptical abutments with armored beds, International Journal of Sediment Research, Vol. 25, Issue 3, pp. 233-245.

KARIMI M., QADERI K., RAHIMPOUR M., AHMADI M. M. (2020). Laboratory Investigation of Effect of Collar on Scour at Bridge Piers Group and Abutment in the Presence of Debris. Irrigation and Drainage Structures Engineering Research, Vol. 21, Issue 78, pp. 99-116.

KASSEM H., EL-MASRY A. A., DIAB R. (2023). Influence of collar's shape on scour hole geometry at circular pier. Ocean Engineering, Vol. 287, pp. 115791.

KHASSAF S. I., AHMED S. I. (2021). Development an empirical formula to calculate the scour depth at different shapes of non-uniform piers, In Journal of Physics: Conference Series, IOP Publishing, Vol. 1973, Issue. 1, pp. 012179.

LANÇA R. M., FAEL C. S., MAIA R. J., PÊGO J. P., CARDOSO A. H. (2013). Clear-water scour at comparatively large cylindrical piers, Journal of Hydraulic Engineering, Vol. 139, Issue11, pp. 1117-1125.

LAURSEN E. M., TOCH A. (1956). Scour around bridge piers and abutments, Vol. 4. Ames, IA: Iowa Highway Research Board.

LI J., GUO Y., LIAN J., WANG H. (2023). Mechanisms, assessments, countermeasures, and prospects for offshore wind turbine foundation scour research. Ocean Engineering, Vol. 281, pp. 114893.

MAZA J. A. (1968). Socavación en cauces naturales. Instituto de Ingenieria, Universidad Nacional Autonoma de Mexico.

MEHTA D.J., YADAV S.M. (2020). Analysis of scour depth in the case of parallel bridges using HEC-RAS, Water Supply, Vol. 20, Issue 8, pp. 3419-3432.

MEHTA D., YADAV S.M., WAIKHOM S., PRAJAPATI K. (2020). Stable channel design of Tapi River using HEC-RAS for Surat Region, Environmental Processes and Management: Tools and Practices, pp. 25-36.

MOWLA Q. A. E., AHMARI H. (2024). Experimental Study of Flow Characteristics and Geometry of Scour Hole around Cylindrical Piers Subject to Wave and Current. Journal of Waterway, Port, Coastal, and Ocean Engineering, Vol. 150, Issue 1, pp. 04023020.

NABIL EL-HAZEK A., ELSAYED METWALLEY W., BADAWY ABDEL-MAGEED N., MOUSSA M. A., AGAHEEN O. (2022). Studying the Shape Effect of Piers on the Vortices in Open Channels, Engineering Research Journal-Faculty of Engineering (Shoubra), Vol. 51, Issue 2, pp. 156-161.

NOVAK P., MOFFAT A. I. B., NALLURI C., NARAYANAN R. A. I. B. (2017). Hydraulic structures. CRC Press.

OKINA S. N., TAILLANDIER F., AHOUET L., HOANG Q. A., BREYSSE D., LOUZOLO-KIMBEMBE P. (2023). Using Conceptual Graph modeling and inference to support the assessment and monitoring of bridge structural health. Engineering Applications of Artificial Intelligence, Vol. 125, pp. 106665

OLIVETO G., HAGER W. H. (2002). Temporal evolution of clear-water pier and abutment scour. Journal of Hydraulic Engineering, Vol. 128, Issue 9, pp. 811-820.

OMARA H., OOKAWARA S., NASSAR K. A., MASRIA A., TAWFIK A. (2022). Assessing local scour at rectangular bridge piers. Ocean Engineering, Vol. 266, pp. 112912.

PAROLA A. C., MAHAVADI S. K., BROWN B. M., EL KHOURY A. (1996). Effects of rectangular foundation geometry on local pier scour. Journal of Hydraulic Engineering, Vol. 122, Issue 1, pp. 35-40.

PIZARRO A., MANFREDA S., TUBALDI E. (2020). The science behind scour at bridge foundations: A review. Water, Vol. 12, Issue 2, pp. 374.

QADERI K., JAVADI F., MADADI M. R., AHMADI M. M. (2021). A comparative study of solo and hybrid data driven models for predicting bridge pier scour depth, Marine Georesources & Geotechnology, Vol. 39, Issue 5, pp. 589-599.

RAFIQUI E. M. A., LONE M. A., TANTRAY M. A. (2023). Scour estimation for hydraulic structures in rivers/streams with coarser bed materials with special reference to Erin stream Bandipora, J&K, India, ISH Journal of Hydraulic Engineering, pp. 1-14.

RAUDKIVI A. J., WITTE H. H. (1990). Development of bed features. Journal of Hydraulic Engineering, Vol. 116, Issue 9, pp. 1063-1079.

RICHARDSON E. V., HARRISON L. J., RICHARDSON J. R., DAVIS S. R. (1993). Evaluating Scour at Bridges, US Department of Transportation, Federal Highway Administration. Hydraulic Engineering Circular, Vol. 18, PP. 01-001.

RICHARDSON E. V., DAVIS S. R. (2001). Evaluating scour at bridges (No. FHWA-NHI-01-001). United States.'Federal Highway Administration. Office of Bridge. Technology.

SETIA B. (2008). Equilibrium scour depth time. In Advanced Topics on Water Resources, Hydraulics and Hydrology. 3rd IASME/WSEAS International Conference on Water Resources, Hydraulics & Hydrology (WHH'08) (pp. 114-117).

SHAHRIAR A. R., ORTIZ A. C., MONTOYA B. M., GABR M. A. (2021). Bridge Pier Scour: An overview of factors affecting the phenomenon and comparative evaluation of selected models. Transportation Geotechnics, Vol. 28, pp. 100549.

SHEN H. W., SCHNEIDER V. R., KARAKI S. S. (1966). Mechanics of local scour. US Department of Commerce, National Bureau of Standards. Institute for Applied Technology.

SHEN H. W., SCHNEIDER V. R., KARAKI S. (1969). Local scour around bridge piers. Journal of the Hydraulics Division, Vol. 95, Issue 6, pp. 1919-1940.

SINGH R. K., PANDEY M., PU J. H., PASUPULETI S., VILLURI V. G. K. (2020). Experimental study of clear-water contraction scour. Water Supply, Vol. 20, Issue 3, pp. 943-952.

TAFAROJNORUZ A., GAUDIO R., DEY S. (2010). Flow-altering countermeasures against scour at bridge piers: a review. Journal of hydraulic research, Vol. 48, Issue 4, pp. 441-452.

TANG H., LIU Q., ZHOU J., GUAN D., YUAN S., TANG L., ZHANG, H. (2023). Process-Based Design Method for Pier Local Scour Depth under Clear-Water Condition. Journal of Hydraulic Engineering, Vol. 149, Issue 12, pp. 06023009.

TISON L. J. (1940). Erosion autour des piles de ponts en riviere. In Annales des Travaux publics de Belgique, Vol. 41, Issue 6, pp. 813-817.

VIJAYASREE B., ELDHO T. (2016). Experimental study of scour around bridge piers of different arrangements with same aspect ratio.

VIJAYASREE B. A., ELDHO T. I., MAZUMDER B. S., AHMAD, N. (2019). Influence of bridge pier shape on flow field and scour geometry. International Journal of River Basin Management, Vol. 17, Issue 1, pp. 109-129.

WANG S., WEI K., SHEN Z., XIANG Q. (2019). Experimental investigation of local scour protection for cylindrical bridge piers using anti-scour collars. Water, Vol. 11, Issue 7, pp. 1515.

WANG R., LEANDER J. (2023). Risk-based decision-making for system-level fatigue assessment of bridges.

XU C., HUANG Z. (2023). A laboratory study of wave-induced local scour at an emergent pile breakwater. Ocean Engineering, Vol. 270, pp. 113618.

YANG Y., MELVILLE B. W., SHEPPARD D. M., SHAMSELDIN A. Y. (2018). Clear-water local scour at skewed complex bridge piers. Journal of Hydraulic Engineering, Vol. 144, Issue 6, pp. 04018019.

ZOLGHADR M., ZOMORODIAN S.M.A., FATHI A., TRIPATHI R.P., JAFARI N., MEHTA D., AZAMATHULLA H.M. (2023). Experimental Study on the Optimum Installation Depth and Dimensions of Roughening Elements on Abutment as Scour Countermeasures, Fluids, Vol. 8, Issue 6.